Available online at www.sciencedirect.com
ScienceDirect
Journal of Molecular Catalysis A: Chemical 269 (2007) 163–168
JOURNAL OF MOLECULAR CATALYSIS A: CHEMICAL
www.elsevier.com/locate/molcata

Manganese(II) halogeno complexes with neutral tris(3,5-diisopropyl-1-pyrazolyl)methane ligand: Synthesis and ethylene polymerization

Masaaki Nabika [a], Seiki Kiuchi [a], Tatsuya Miyatake [a,*], Ken-Ichi Okamoto [b], Kiyoshi Fujisawa [b,**]

[a] *Petrochemicals Research Laboratory, Sumitomo Chemicals Co. Ltd., 2-1 Kitasode, Sodegaura, Chiba 299-0295, Japan*
[b] *Graduate School of Pure and Applied Sciences, University of Tsukuba, 1-1-1 Tennodai, Tsukuba, Ibaraki 305-8571, Japan*

Received 5 October 2006; received in revised form 23 December 2006; accepted 29 December 2006
Available online 17 January 2007

Abstract

Manganese(II) halogeno complexes containing a neutral tris(3,5-diisopropyl-1-pyrazolyl)methane (referred to as L1′) ligand have been examined on their catalytic performance in ethylene polymerization and ethylene/1-hexene copolymerization. The activities of [Mn(Cl_2)(L1′)] (**a**) and [Mn(Br)(L1′)](Br) (**b**) activated by Al(*i*-Bu)$_3$/(Ph_3C)[B(C_6F_5)$_4$] for ethylene polymerization go up to 1600 and 840 kg mol (cat)$^{-1}$ h^{-1} with a bimodal molecular weight distribution (M_w/M_n) of 4.1 and 4.2, respectively. These results are different from the corresponding manganese(II) complexes with hydrotris(pyrazolyl)borate anion.

Keywords: Manganese complex; Tris(pyrazolyl)methane; Polymerization reaction; Ethylene; 1-Hexene

1. Introduction

The highly active group 4 metallocene catalysts have developed into new single-site catalysts by using the well-defined organometallic and inorganic compounds [1–5]. Hydrotris(pyrazolyl)borate (Tp) ligands are attractive candidate ligands for single-site catalysts [6]. Tp ligands are formally analogous to cyclopentadienyl (Cp) ligands in which both are six-electron donor minus one ligands [7,8]. Tp ligands are three-fold symmetric σ-N donors and tend to form facial type octahedral complexes, while Cp ligands are typically five-fold symmetric π-C donors and tend to form tetrahedral complexes. Several studies demonstrated that TpTiCl_n(OR)$_{3-n}$/methylaluminoxane (MAO) catalysts (n = 1–3) containing the simple Tp ligands, HB(pz)$_3^-$ (pzH = pyrazole) or HB(3,5-Me_2pz)$_3^-$, polymerize ethylene, ethylene/α-olefins, and styrene [9,10]. However, these catalysts exhibit poor activity and produce polymers with broad molecular weight distributions. Recently, Jordan and co-workers reported the ethylene polymerization behavior of a set of TpTiCl_3 and TpTiCl_2(OR) complexes with sterically crowded ligands such as HB(3-mesitylpz)$_3^-$ (TpMs) or HB(3-mesitylpz)$_2$(5-mesitylpz)$^-$ (TpMs*) under MAO activation conditions [11]. They showed that the activity of TpTiX_3/MAO catalysts was strongly influenced by the Tp steric properties. In particular, the bulky TpMs- and TpMs*-based catalysts exhibited high activity producing linear polyethylene (PE). Michiue and Jordan also reported that the closely related Ti^{III} catalyst K[TpMs*$Ti^{III}Cl_3$] behaved somewhat differently compared with TpMs*$Ti^{IV}Cl_3$ under MAO activation conditions [12] and that TpMCl_3 (M = Zr or Hf) complexes showed extremely high activity for ethylene polymerization and ethylene/1-hexene copolymerization [13].

Although many efforts have been made to survey new transition metal complex catalysts [2–4], less attention has been paid to group 7 metal catalysts. Mn-based catalysts would be expected to have unique features different from either early or late transition metal catalysts. Ban and co-workers revealed that Mn^{III}(acac)$_3$, Cp_2Mn^{II}, and Mn^{III}(salen)Cl were effective for

* Corresponding author. Tel.: +81 436 61 5374; fax: +81 436 61 5344.
** Corresponding author. Tel.: +81 29 853 6922; fax: +81 29 853 6503.
E-mail addresses: miyataket1@sc.sumitomo-chem.co.jp (T. Miyatake), kiyoshif@chem.tsukuba.ac.jp (K. Fujisawa).

1381-1169/$ – see front matter © 2007 Elsevier B.V. All rights reserved.
doi:10.1016/j.molcata.2006.12.043

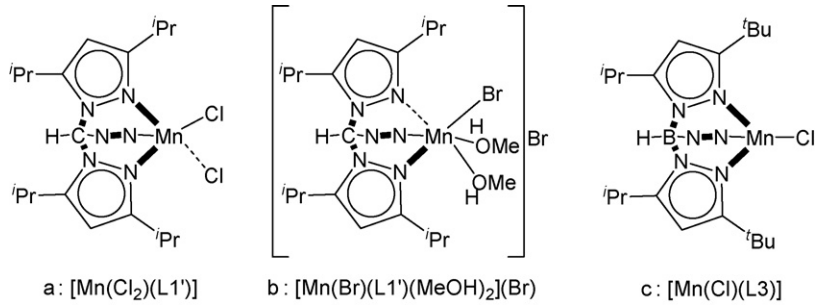

Fig. 1. Manganese(II) complexes used for this research. N—N represents the third, hidden pyrazolyl group.

ethylene polymerization, but only trace amounts of polymers were isolated when MAO was used as an activator [14]. In their report, linear PE having relatively narrow molecular weight distribution ($M_w/M_n = 2.8$) was only obtained. Moreover, Gibson and co-workers indicated that manganese(II) chloro complex with bis(imino)pyridine showed much lower ethylene polymerization activity than the related Fe^{II}, Co^{II}, and V^{III} complexes [2,3]. The poor catalytic activity was explained by reductive alkylation to form Mn^{I} and Mo^{o} alkyl complexes, $[Mn^{I}(CH_3)(L)]$ and $[Li(OEt)_4][Mn^{o}(CH_2SiMe_3)(L)]$ (L = 2,6-bis[1-(2,6-diisopropylphenylimino)ethyl]pyridine), respectively [15].

Recently, we demonstrated that Mn^{II}-based complexes, [Mn(X)(L3)] (X = Cl, Br, or NO_3; $L3^-$ = hydrotris(3-tertiary butyl-5-isopropyl-1-pyrazolyl)borate anion) could compete with the general metallocene catalyst systems, having relatively narrow molecular weight distribution ($M_w/M_n = 1.8$) [16]. In this paper, we report syntheses and characterizations of manganese(II) halogeno complexes (**a** and **b**) with a neutral tris(3,5-diisopropyl-1-pyrazolyl)methane ($HC(3,5\text{-}i\text{-}Pr_2pz)_3$ ligand, referred to as L1′) and the polymerization reaction of ethylene and ethylene/1-hexene under activation conditions, as compared with the related manganese(II) chloro complex (**c**) with the anionic borate ligand $L3^-$ (Fig. 1); some differences in structures and properties of copper(I) complexes between anionic hydrotris(pyrazolyl)borate ligands and neutral tris(pyrazolyl)methane ligands have been observed [17].

2. Experimental

2.1. Materials

Preparation and handling of all complexes were performed under an argon or nitrogen atmosphere using the standard Schlenk tube techniques or a glovebox. Dichloromethane was distilled from phosphorous pentaoxide prior to use. Diethyl ether was carefully purified by refluxing/distilling under an argon atmosphere over sodium benzophenone ketyl [18]. Methanol of spectroscopic grade was used after bubbling with an argon gas. Toluene was dehydrated with activated alumina and was deoxygenated by bubbling with a dried nitrogen gas before use. Other reagents were commercially available and used without further purification. The ligand for present research L1′ was prepared according to the published methods [17,19]. Triisobutylaluminum (TIBA) (1 mol Al/L solution in toluene) and modified methylaluminoxane (MMAO) (2.1 mol Al/L solution in toluene) were purchased from Tosoh Finechem. Co. Ltd. (referred to as MMAO-3A). Triphenylcarbenium tetrakis(pentafluorophenyl)borate (TB) was purchased from Asahi Glass Co. Ltd. and used as 0.0050 mol/L toluene solution. Manganese complexes $[Mn(Cl_2)(L1')]$ (**a**) and [Mn(Br)(L1′)](Br) (**b**) were dissolved in toluene to give 2.0 mmol/L solution for polymerization use.

2.2. Instrumentation

IR and far-IR spectra for complex characterizations were recorded on KBr pellets in the 4000–400 cm^{-1} region and on CsI pellets in the 650–150 cm^{-1} region using a JASCO FT/IR-550 spectrophotometer, respectively. Abbreviations used in the description of vibration data are as follows: vs, very strong; s, strong; m, medium; w, weak. The elemental analyses (C, H, N) were performed at the Department of Chemistry of the University of Tsukuba.

The structure of the copolymer obtained was examined by a ^{13}C NMR spectroscopy (62.9 MHz) using a Bruker AC spectrometer operating at 135 °C. The copolymer sample was prepared in sample tubes 10 mm in diameter by dissolving 250 mg of the polymer in 3.0 mL of *o*-dichlorobenzene containing 0.3 mL of *o*-dichlorobenzene-d_4 [20].

Molecular weight (M_w and M_n) and molecular weight distribution (M_w/M_n) was determined by high temperature GPC and calibrated using polystyrene standards. GPC analysis was performed with a HLC-8121GPC/HT liquid chromatograph at 152 °C in *o*-dichlorobenzene using a TSK-GEL GMHHR-H(20)HT column. Differential scanning calorimetry (DSC) melting curves were recorded at a rate of 5 °C/min using a Seiko SSC-5200. The melting point (T_m) of copolymers was measured from the second heating.

2.3. Synthesis of Mn-complexes

2.3.1. $[Mn(Cl_2)(L1')]$ (*a*)

To the solution of $MnCl_2{\cdot}4H_2O$ (0.390 g, 1.97 mmol) in 30 mL of methanol was added the solution of L1′ (1.01 g, 2.17 mmol) in 30 mL of dichloromethane. After the mixture was stirred at room temperature for 3 h, the solvent was removed in vacuo. The resultant white powder was recrystallized from dichloromethane/diethyl ether at −30 °C, and colorless crystals were formed. Yield 71% (0.825 g). Anal. calcd. for

$C_{28}H_{46}N_6MnCl_2$: C, 56.76%; H, 7.83%; N, 14.18%. Found: C, 56.46%; H, 7.99%; N, 13.98%. IR (cm^{-1}): 2965vs, 2929s, 2867s, 1556s, 1469vs, 1383s, 1305s, 1243m, 1181m, 1061m, 1011m, 828s, 805m, 673m. Far-IR (cm^{-1}): 590m, 521m, 457w, 391w, 341w, 280s, 192w, 156w.

2.3.2. [Mn(Br)(L1′)]Br (**b**)

The synthesis was carried out by the same method as **a** using L1′ (1.01 g, 2.17 mmol) and $MnBr_2{\cdot}4H_2O$ (0.566 g, 1.97 mmol). Yield 73% (0.983 g). Anal. calcd. for $C_{28}H_{46}N_6MnBr_2$: C, 49.35%; H, 6.80%; N, 12.33%. Found: C, 49.20%; H, 6.89%; N, 12.17%. IR (cm^{-1}): 2965vs, 2928s, 2867s, 1556s, 1469vs, 1383s, 1305s, 1243m, 1181m, 1060s, 1011w, 829s, 806w, 672m. Far-IR (cm^{-1}): 590m, 522m, 458w, 393w, 305w, 281w, 235m 205s, 181w.

2.4. Typical ethylene polymerization experiment

An autoclave having an inner volume of 400 mL was dried under vacuum, and then purged with argon. After charged with 200 mL of toluene, the autoclave was heated to 60 °C. Then, ethylene was fed while the ethylene pressure was adjusted at 2.0 MPa. After the system was stabilized, 1.0 mmol of MMAO was added to the mixture. Subsequently 10 μmol of **a** was added. Polymerization was carried out for 60 min while the temperature was kept at 60 °C. The polymerization reaction was quenched by the addition of 5 mL of methanol. After a few minutes, the gas was vented and the reaction mixture was then poured into 400 mL of methanol with 5 mL of hydrochloric acid (1 mol/L). The obtained polymer was collected by filtration and washed with flesh methanol, and dried in a high vacuum at 80 °C for 8 h.

2.5. Typical ethylene/1-hexene copolymerization experiment

An autoclave having an inner volume of 400 mL was dried under vacuum, after then purged with argon. After charged with 2–50 mL of 1-hexene and 198–150 mL of toluene (total liquid volume is 200 mL), the autoclave was heated to 60 °C. After heating, ethylene was fed while the ethylene pressure was adjusted at 2.0 MPa. After the system was stabilized, 0.25 mmol of TIBA was added to the mixture. Subsequently 1.0 μmol of **a** and 3.0 μmol of TB were added. Polymerization was carried out for 60 min while the temperature was kept at 60 °C. The polymerization reaction was quenched by the addition of 5 mL of methanol. A few minutes later, the gas was vented and the reaction mixture was then poured into 400 mL of methanol with 5 mL of hydrochloric acid (1 mol/L). The obtained copolymer was collected by filtration and washed with flesh methanol, and dried in a high vacuum at 80 °C for 8 h.

2.6. X-ray structure determination

Crystal data and refinement parameters for **a** and **b** are given in Table S1. The diffraction data for both complexes were measured on a Rigaku/MSC Mercury CCD system with graphite monochromated Mo Kα (λ = 0.71069 Å) radiation at low temperature (−66 °C for **a** and −69 °C for **b**). Each crystal was mounted on the tip of a glass fiber by heavy-weight oil. The unit cell parameters of each crystal from six image frames were retrieved using Rigaku Daemon software and refined using CrystalClear on all observed reflection [21]. Data using 0.5° intervals in ϕ and ω for 30 s/frame were collected with a maximum resolution of 0.77 Å (744 oscillation images). The data were corrected for Lorentz and polarization effects. An empirical absorption correction was applied to each complex [21–23]. Structures were solved by direct-methods (SIR 92) [24]. The positions of the metal atoms and their first coordination sphere were located from the E-map; other non-hydrogen atoms were found in alternating difference Fourier syntheses [25]. Least-squares refinement cycles were refined anisotropically during the final cycles (CrystalStructure) [24,25]. Hydrogen atoms were placed in calculated positions. Strong remaining peaks are due to the disordered molecules. In **a**, one of two chlorine atoms coordinated to Mn^{II} ion is disordered over two positions, each with half-occupancy. The disordered CH_3 groups (C12 and C12′) were also refined with a site occupancy factor of 0.5.

3. Results and discussion

3.1. Structures of manganese(II) complexes *a* and *b*

The sterically crowded tris(pyrazolyl)methane ligand L1′ was synthesized by the reaction between 3,5-diisopropylpyrazole and $CHCl_3$ [16,18]. The reaction of L1′ with 0.9 equiv. of $MnCl_2{\cdot}4H_2O$ and $MnBr_2{\cdot}4H_2O$ in a mixed solvent MeOH/CH_2Cl_2 (1:1) gave colorless powder as [Mn(Cl_2)(L1′)] (**a**) and [Mn(Br)(L1′)](Br) (**b**) in higher yields (∼70%), respectively (Fig. 1).

The molecular structures of **a** and **b** were determined by X-ray diffraction, showing different six-coordinated structures (Appendix B and Figs. S1 and 2). In **a**, two chloride ions coordinate to Mn^{II} ion, one sets of them being disordered having each half-occupancy with *Pnma* symmetry. Two Mn^{II}–Cl distances are not equivalent: 2.326(4) Å (Mn1–Cl1) versus 2.646(5) Å (Mn1–Cl_2(′)). That is to say, the disordered chlorine atoms (Cl_2(′)) coordinate weakly to Mn^{II} ion (Table S2). In comparison with the related manganese(II) chloro complexes **c**, the stronger coordinated Mn–Cl distance of 2.326(4) Å in **a** is longer than the Mn–Cl distance of 2.287(1) Å in **c**. In **b**, one of bromide ions and two MeOH molecules coordinate to Mn^{II} ion, having a distorted octahedral geometry. The stronger coordinated Mn–Cl distance in **a** is shorter than the Mn–Br distance of 2.5682(10) Å in **b**. Moreover, the Mn–N21 distance of 2.313(4) Å in **b** is slightly longer than others because of steric hindrance. In summary, the coordination geometries of complexes **a** and **b** are clearly different from the coordination geometry of **c**. It may come from the different total charge of the supporting ligands (neutral in **a** and **b** and minus one in **c**) and/or the different geometries (six-coordination in **a** and **b** and four-coordination in **c**).

3.2. Ethylene homopolymerization behavior

The results of ethylene polymerization reaction with manganese(II) halogeno complexes (**a**, **b**, and **c**) are summarized

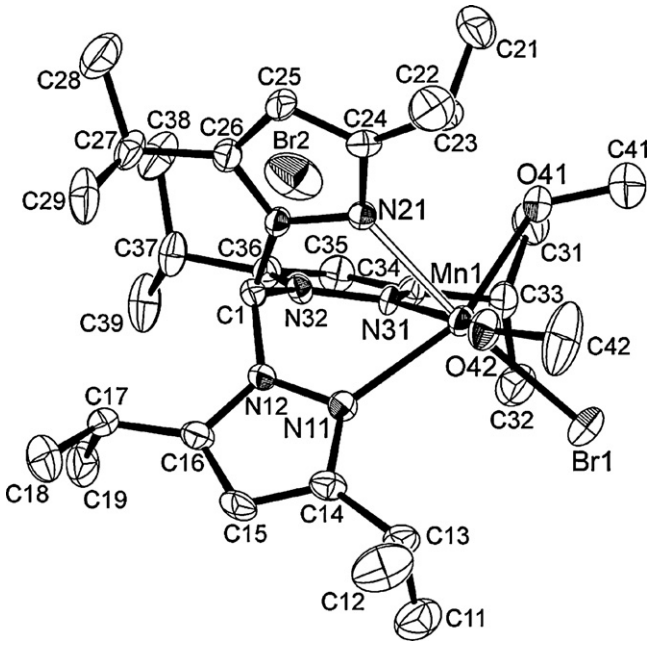

Fig. 2. Molecular structure (50% probability ellipsoids) of complex **b**·$(MeOH)_2$. The solvents and the hydrogen atoms are omitted for clarity.

in Table 1. In all cases, the ethylene polymerization activity of **a** and **b** activated by TIBA/TB(II) was greater than that activated by MMAO(I). This tendency was the same as the related manganese(II) chloro complex **c** with the anionic borate ligand [16]. In particular, when MMAO was used as an activator, a negligible weight of polymer was obtained (Table 1, entries 1 and 3). On the other hand, when activated by TIBA/TB(II), the chloro complex **a** showed higher catalytic activity of 1600 kg mol $(cat)^{-1}$ h^{-1} than the bromo complex **b** (840 kg mol $(cat)^{-1}$ h^{-1}) for polymerization of ethylene at 60 °C under 2.0 MPa of ethylene pressure (Table 1, entries 2 and 4). The activity of **a** is far superior to that of **c** (920 kg mol $(cat)^{-1}$ h^{-1}). Manganese(II) catalysts with the present neutral methane ligand system produce PE having broad molecular weight distribution (M_w/M_n: 4.1 in **a** and 4.2 in **b**), which is different from the case of **c** with the anionic borate ligand, having narrow molecular weight distribution (M_w/M_n: 2.3). Moreover, the PEs produced from **a** and **b** show higher molecular weights (356×10^3 and 343×10^3, respectively), approximately four times the molecular weight of PE produced from **c** (96×10^3). These results indicate that the active species of **a** and **b** are the same and are different from those of **c**. In order to shed light on this different reaction behavior, we also examined ethylene/1-hexene copolymerization reaction (see next section).

3.3. Ethylene/1-hexene copolymerization behavior

The catalyst systems of **a** and **b** activated by TIBA/TB(II) copolymerized ethylene and 1-hexene. As shown in Table 2, the copolymerization was conducted under the same conditions as those for entry 1 in Table 1 except that 198 mL of toluene and 2 mL of 1-hexene were used instead of 200 mL of toluene. These catalytic activities of both **a**/TIBA/TB and **b**/TlBA/TB were decreased gradually with an increase in the concentration of 1-hexene. The molecular weight of these copolymers was decreased by degrees with an increase in the concentration of 1-hexene (Table 2, entries 7–14). These results suggest that the polymer forms at the dormant site from insertion of 1-hexene to the active species. The dependence of molecular weight of copolymers on the concentration of 1-hexene was similar to that of ethylene–α-olefin copolymer produced from group 4 metallocene with co-catalyst [26].

It seems that 1-hexene was incorporated more efficiently by **a** and **b** than by **c**. The 1-hexene content using **a** with 10 mL of 1-hexene fed (2.1 mol%, entry 8) was more than that using **c** with 30 mL of 1-hexene fed (1.6 mol%, entry 17), as shown in Fig. 3. In addition, the resultant poly(ethylene-co-1-hexene)s produced from **a** and **b** possessed relatively higher molecular weights than those produced from **c**. However, these polymers had bimodal molecular weight distributions confirmed by GPC traces as shown in Fig. 4 (**a** and **b**: $M_w = (212–326) \times 10^3$, $M_w/M_n = 2.5–3.8$; **c**: $M_w = (57–62) \times 10^3$, $M_w/M_n = 1.7–1.9$).

As described above, the polymerization behavior of **a** and **b** was similar but different from that of **c** (Table 2, entries 15–18). Therefore, active species with similar structure would be formed from **a** and **b**. However, polymerization activities were slightly different. It is assumed the coordinated halides (i.e., Mn–Cl or Mn–Br) or the free anions (i.e., Cl^- or Br^-) would have some influence on polymerization reactions.

Table 1
Polymerization of ethylene catalyzed by manganese(II) complexes with co-catalysts[a]

Entry	Catalyst	Co-catalyst[b]	Activity[c]	M_w[d] ($\times 10^{-3}$)	M_w/M_n[d]	T_m (°C)
1	**a**	I	0			
2		II	1600	356	4.1	135.9
3	**b**	I	Trace			
4		II	840	343	4.2	136.2
5[e]	**c**	I	11	64	1.9	–
6[e]		II	920	96	2.3	135.5

[a] Conditions: 0.4 L autoclave, ethylene 2.0 MPa, polymerization time 60 min, temperature 60 °C; solvent: toluene = 200 mL.
[b] (I) Catalyst 1.0 μmol, MMAO-3A 1.0 mmol. (II) Catalyst 1.0 μmol, TIBA 1.0 mmol, TB 3.0 μmol.
[c] In kg mol $(cat)^{-1}$ h^{-1}
[d] Determined by GPC with polystyrene standards.
[e] Ref. [16].

Table 2
Copolymerization of ethylene and 1-hexene catalyzed by manganese(II) complexes with TIBA/TB[a]

Entry	Catalyst	[1-Hexene] (mL)	Activity[b]	M_w[c] ($\times 10^{-3}$)	M_w/M_n[c]	T_m (°C)	1-Hexene content[d]
7	**a**	2	1350	326	3.3	120.6	0.82
8		10	1200	292	3.4	108.4	2.12
9		30	880	251	2.7	81.4	5.44
10		50	780	212	2.5	65.8	7.87
11	**b**	2	820	312	3.8	121.2	0.71
12		10	940	292	3.3	108.7	2.05
13		30	860	258	2.6	87.4	5.63
14		50	760	227	2.5	71.7	8.04
15[e]	**c**	2	6700	58	1.8	132.8	0.23
16[e]		10	3130	61	1.7	127.7	0.61
17[e]		30	2090	62	1.7	116.4	1.60
18[e]		50	720	57	1.9	113.7	2.55

[a] Conditions: 0.4 L autoclave, ethylene 2.0 MPa, polymerization time 60 min, temperature 60 °C; **a**, **b** or **c** 1.0 μmol, TIBA 1.0 mmol, TB 3.0 μmol; solvent: toluene + 1-hexene = 200 mL.
[b] In kg mol (cat)$^{-1}$ h^{-1}.
[c] Determined by GPC with polystyrene standards.
[d] mol%, determined by ^{13}C NMR spectroscopy.
[e] Ref. [16].

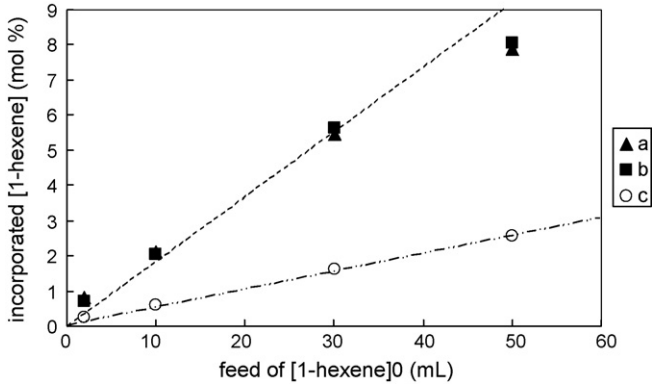

Fig. 3. 1-Hexene content of ethylene/1-hexene copolymers vs. feed of 1-hexene.

The separations of broad peaks of GPC curves for entries 2, 8, and 10 were carried out (Fig. 5). Lower molecular weight peaks scarcely changed with 1-hexene incorporation and higher peaks markedly changed with it. In other words, these systems were combined by more than two active species. We cannot identify these species; however, it is estimated that these are two types of coordination species with tridentate and bidentate ligations because of the relatively weak Mn–N coordination bond in **a** and **b**. Since the Mn–N bond distances of **c** are shorter than those in **a** and **b** according to the X-ray structural analysis, complex **c** would keep its tridentate coordination sphere in the catalytic reaction. Therefore complex **c** produced PEs with monomodal and narrow molecular weight distribution. The inspection of polymerization behavior of manganese(II) halogeno complexes with neutral bidentate ligands such as bis(pyrazolyl)methane would be needed for further consideration.

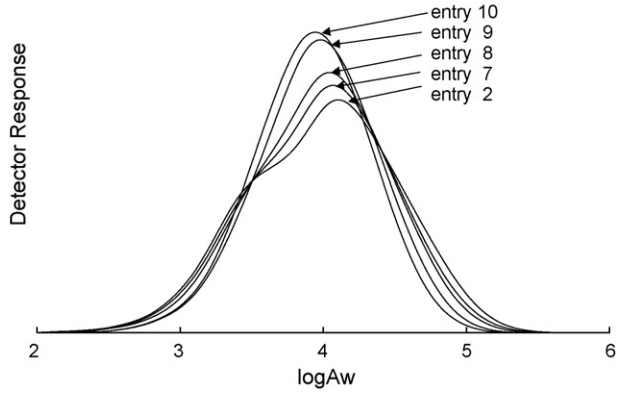

Fig. 4. GPC traces of the ethylene–1-hexene copolymers produced from **a**/TIBA/TB.

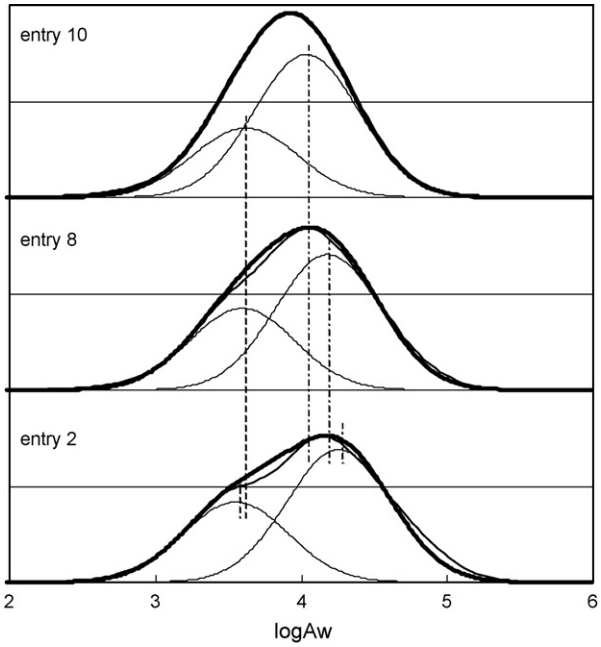

Fig. 5. Segmentation of GPC curves into two normal distribution curves.

These manganese(II) complexes with the neutral tridentate methane ligand have a six-coordinated structure, as determined by X-ray structural analysis. Moreover, manganese complex can be converted to alkyl manganese species [15,27,28]. Thus, it is assumed that the polymerization on this manganese catalyst follows a mechanism similar to that of the polymerization on group 4 metallocene catalysts. As mentioned in Introduction, the high catalytic activity could be obtained by avoiding reductive alkylation reaction. These manganese(II) catalysts with the neutral methane ligand would not be reduced during polymerization reactions. Further studies concerning the structure of the actual active species and the effect of auxiliary ligands are currently in progress.

Acknowledgments

We thank Mr. Takashi Kohara for NMR analysis and Ms. Hiroko Hirahata and Mr. Mitsuharu Mitobe for GPC analysis. This research was in part supported by Grant-in-Aid for Scientific Research (B) (nos. 13555257, 14350471, and 17350043) from the Japan Society for the Promotion of Science and the 21st Century COE Program from the Ministry of Education, Culture, Sports, Science and Technology to KF.

Appendix A. Supplementary data

Tables of crystallographic details (Table S1), selected bond distances and angles (Table S2), and molecular structure of **a** (Fig. S1) are available. Crystallographic data (excluding structure factors) for the two structures reported in the present paper have been deposited at the Cambridge Crystallographic Data Centre and allocated the deposition numbers CCDC 614938–614939. These data can be obtained free of charge via http://www.ccdc.ac.uk/conts/retrieving.html or on application to CCDC, Union Road, Cambridge CB2 1EZ, UK [fax: +44 1223 336033, e-mail: deposit@ccdc.cam.ac.uk]. Supplementary data associated with this article can be found, in the online version, at doi:10.1016/j.molcata.2006.12.043.

References

[1] W. Kaminsky, Macromol. Chem. Phys. 197 (1996) 3907–3945.
[2] V.C. Gibson, S.K. Spitzmesser, Chem. Rev. 103 (2003) 283–315.
[3] G.J.P. Britovsek, V.C. Gibson, D.F. Wass, Angew. Chem. Int. Ed. 38 (1999) 428–447.
[4] S.D. Ittel, L.K. Johnson, M. Brookhart, Chem. Rev. 100 (2000) 1169–1203.
[5] M. Mitani, J. Saito, S. Ishii, Y. Nakayama, H. Makio, N. Matsukawa, S. Matsui, J. Mohri, R. Furuyama, H. Terao, H. Bando, H. Tanaka, T. Fujita, Chem. Recd. 4 (2004) 137–158.
[6] S. Trofimenko, Scorpionates: The Coordination Chemistry of Polypyrazolylborate Ligands, Imperial College Press, London, 1999.
[7] N. Kitajima, W.B. Tolman, Prog. Inorg. Chem. 43 (1995) 419–531.
[8] D.M. Tellers, S.J. Skoog, R.G. Bergman, T.B. Gunnoe, W.D. Harman, Organometallics 19 (2000) 2428–2432.
[9] A. Karam, M. Jimeno, J. Lezama, E. CatarÍ, A. Figueroa, B.R. de Gascue, J. Mol. Catal. A 176 (2001) 65–72.
[10] H. Nakazawa, S. Ikai, K. Imaoka, Y. Kai, T. Yano, J. Mol. Catal. A 132 (1998) 33–41.
[11] S. Murtuza, O.L. Casagrande Jr., R.F. Jordan, Organometallics 21 (2002) 1882–1890.
[12] K. Michiue, R.F. Jordan, Macromolecules 36 (2003) 9707–9709.
[13] K. Michiue, R.F. Jordan, Organometallics 23 (2004) 460–470.
[14] H.T. Ban, T. Kase, M. Murata, J. Polym. Sci. A: Polym. Chem. 39 (2001) 3733–3738.
[15] D. Reardon, G. Aharonian, S. Gambarotta, G.P.A. Yap, Organometallics 21 (2002) 786–788.
[16] M. Nabika, Y. Seki, T. Miyatake, Y. Ishikawa, K. Okamoto, K. Fujisawa, Organometallics 23 (2004) 4335–4337.
[17] K. Fujisawa, T. Ono, Y. Ishikawa, N. Amir, Y. Miyashita, K. Okamoto, N. Lehnert, Inorg. Chem. 45 (2006) 1698–1713.
[18] W.L.F. Armarego, D.D. Perrin, Purification of Laboratory Chemicals, 4th ed., Butterworth/Heinemann, Oxford, UK, 1997.
[19] K. Fujisawa, T. Ono, H. Aoki, Y. Ishikawa, Y. Miyashita, K. Okamoto, H. Nakazawa, H. Higashimura, Inorg. Chem. Commun. 7 (2004) 330–332.
[20] M. de Pooter, P.B. Smith, K.K. Dohrer, K.F. Bennet, M.D. Meadows, C.G. Smith, H.P. Schouwenaars, R.A. Geerards, J. Appl. Polym. Sci. 42 (1991) 399–408.
[21] J.W. Pflugrath, CrystalClear Ver. 1.3, Acta Crystallogr., Sect. D 55 (1999) 1718–1725.
[22] CrystalStructure 3.70: Crystal Structure Analysis Package, Rigaku and Rigaku/MSC, 2000–2005.
[23] D.J. Watkin, C.K. Prout, J.R. Carruthers, P.W. Betteridge, Crystal Issue 10, Chemical Crystallography Laboratory, Oxford, UK, 1996.
[24] SIR 92: A. Altomare, G. Cascarano, C. Giacovazzo, A. Guagliardi, J. Appl. Crystallogr. 26 (1993) 343–350.
[25] P.T. Beurskens, G. Admiraal, G. Beurskens, W.P. Bosman, R. de Gelder, R. Israel, J.M.M. Smits, DIRDIF-99, Technical Report of the Crystallography Laboratory, University of Nijmegen, The Netherlands, 1999.
[26] J. Suhm, M.J. Schneider, R. Mülhaupt, J. Mol. Catal. A: Chem. 128 (1998) 215–227.
[27] J. Chai, H. Zhu, H. Fan, H.W. Roesky, J. Magull, Organometallics 23 (2004) 1177–1179.
[28] S.C. Bart, E.J. Hawrelak, A.K. Schmisseur, E. Lobkovsky, P.J. Chirik, Organometallics 23 (2004) 237–246.